Available online at www.sciencedirect.com
ScienceDirect
Surface & Coatings Technology 202 (2008) 2403–2407
SURFACE & COATINGS TECHNOLOGY
www.elsevier.com/locate/surfcoat

Structural and Mechanical properties of Ti–Si–C–ON for biomedical applications

Freddy Guimarães [a], Cristina Oliveira [a], Elsa Sequeiros [a], Marta Torres [a], M. Susano [b], M. Henriques [b], R. Oliveira [b], R. Escobar Galindo [c], S. Carvalho [a,*], N.M.G. Parreira [d], F. Vaz [a], A. Cavaleiro [d]

[a] Dept. Física, Universidade do Minho, Campus de Azurém, 4800-058 Guimarães, Portugal
[b] IBB—Institute for Biotechnology and Bioengineering Centre for Biological Engineering, Universidade do Minho, Campus de Gualtar, 4700-057, Portugal
[c] Instituto de Ciencia de Materiales de Madrid (ICMM-CSIC), Cantoblanco, 28049, Madrid, Spain
[d] ICEMS—Fac. de Ciências e Tecnologia da Universidade de Coimbra, 3030-788 Coimbra, Portugal

Available online 4 September 2007

Abstract

Ti–Si–C–ON films were deposited by DC reactive magnetron sputtering using different partial pressure of oxygen (p_{O2}) and nitrogen (p_{N2}) ratio. Compositional analysis revealed the existence of two different growth zones for the films; one zone deposited under low p_{O2}/p_{N2} and another zone deposited under high p_{O2}/p_{N2}. The films produced under low p_{O2}/p_{N2} were deposited at a lower rate and presented a fcc structure, as well as, dense and featureless morphologies. The films deposited with high p_{O2}/p_{N2}, consequently higher oxygen content, were deposited at a higher rate and developed an amorphous structure. The structural changes are consistent with the hardness and Young's modulus evolution, as seen by the significant reduction of the hardness and influence on the Young's modulus by increasing p_{O2}/p_{N2}.

Keywords: Ti–Si–C–ON; Mechanical; Structural; Biomaterials

1. Introduction

Significant development of nanotechnology in material science and engineering has taken place in the last decade. The recent interest in the so-called *multifunctional-coating* materials is of major importance, from both the fundamental scientific viewpoint and in terms of industrial applications. More specifically nowadays, as the tendency in implant science is to substitute the total hip replacement, usually a variety of materials, such as metals, ceramics, polymers and composites by materials coated with protective thin-films [1]. Clinical results show that excessive wear and wear debris are the primary cause of failure implants of ultra high molecular weight polyethylene—UHMWPE or metal [2]. Moreover, infections caused by commensal microrganisms are also a cause of implant failure. For example, *Staphylococcus epidermidis* and other coagulase-negative staphylococci (CoNS) are amongst the major culprits for these infections [3,4]. This is related, in part, to their ability to adhere to implanted medical devices and form biofilms. Despite several efforts to find medical therapies to treat biofilm infections [5], the physical removal of an infected medical device is often necessary with its associated inconvenience and additional economic cost. There is considerable interest in increasing the lifetime of implants through the inhibition of biofilm formation and the use of more wear-resistant biocompatible coatings.

The purpose of this work is to start to investigate the feasibility of various Ti–Si–C–ON films for load-bearing medical devices. From known results it is widely accepted that is possible to achieve superhardness by Si incorporation in TiN [6] and a decrease in the Young's modulus is observed by addition of oxygen [7]. Also, work has shown that the corrosion resistance tends to be slightly improved by oxygen incorporation [8]. Recent published works showed that Ti–Si–C is a promising system because of its particular structure, as well as, its extraordinary mechanical and tribological properties [9].

* Corresponding author.
E-mail address: nocas@fisica.uminho.pt (S. Carvalho).

0257-8972/$ - see front matter © 2007 Elsevier B.V. All rights reserved.
doi:10.1016/j.surfcoat.2007.08.056

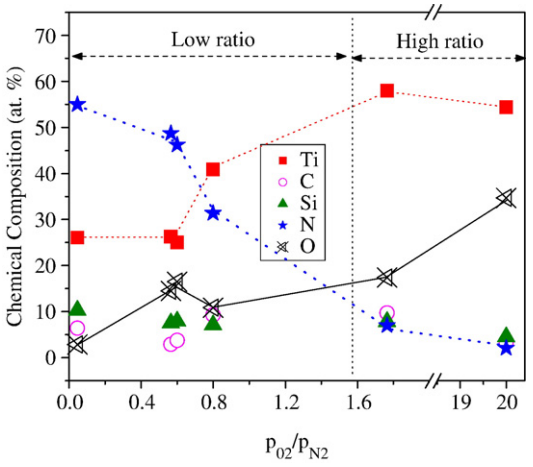

Fig. 1. Variation of the concentration of Ti, C, Si, O and N as a function of p_{O2}/p_{N2}.

Taking this into consideration, the main task of this paper is focussed on the study of the structural and mechanical properties of Ti–Si–C–ON films with different O/N ratios.

2. Experimental details

The Ti–Si–C–ON samples were deposited by d.c. reactive magnetron sputtering from two opposed high purity (99.6%) Ti targets (20×10 cm^2); one Ti target with some incrusted Si pellets (hereafter designated as the TiSi target) and the other with carbon pellets (designated as the TiC target), placed in preferential eroded zone. The area occupied by the pellets was close to 11 cm^2 in each target. Depositions were carried out under an Ar+(N_2+O_2) atmosphere in an Alcatel SCM 650 apparatus. During the depositions the substrates (steel and silicon) were rotated 70 mm above the target at constant speed of 7 rpm. The base pressure in the chamber was about 10^{-4} Pa and rose 4.5×10^{-1} Pa during the depositions.

In order to change the amount of oxygen, the samples were grown with a variation in the N_2+O_2 flow (changing the N_2 from 6.5 to 0 sccm and the O_2 from 0 to 5.25 sccm), while maintaining the Ar flow constant at 60 sccm. The substrate bias voltage and the temperature were kept constant at −50 V and 200 °C, respectively. The current density applied to the TiC target was 5 mA/cm^2 and that to the TiSi target was 6 mA/cm^2.

Electron Probe MicroAnalysis (EMPA) and Glow Discharge Optical Emission Spectroscopy (GDOES) were used for the determination of the chemical composition of the coatings and were carried out using a Cameca SX-50 electron probe microanalysis apparatus and a Jobin Yvon RF GD Profiler, respectively. The cross-sectional morphology was examined using a conventional SEM on fractured samples. The structure and phase composition of the coatings were assessed by XRD, using a conventional Philips PW 1710 diffractometer, operating with CuK_α radiation, in a Bragg-Brentano configuration. The hardness (H) and the Young's modulus (E), were evaluated by depth-sensing indentation, using a Fisherscope H100 apparatus at maximum load of 30 mN. Correction of the geometrical defects in the tip of the indenter, thermal drift of the equipment and uncertainty of the initial contact was also performed in agreement with what is proposed on [10,11]. It should be pointed out that any correction due to residual stresses was done. The Residual stresses, σ_r, were obtained by the deflection method from Stoney's equation [12], using substrate curvature radii, both before and after coating deposition [13].

3. Results and discussion

3.1. Composition morphology analysis

The chemical analysis of the films was obtained using GDOES and EPMA measurements. For the deposited samples the results of an average of these analyses as function of the oxygen partial pressure and the nitrogen partial pressure ratio (p_{O2}/p_{N2}) are shown in Fig. 1. It is visible that the Si and C content remains almost constant for all coatings independent of p_{O2}/p_{N2} and the value is very low (<10 at.%). As expected, the nitrogen content decreased from 54 to 2 at. % and the oxygen increased from 2.9 to 34.7 at. % on increasing the p_{O2}/p_{N2} from 0.046 to 20. Also an increase in Ti content was observed as p_{O2}/p_{N2} increased. In fact, due to the high amount of nitrogen in the coating deposited with lower p_{O2}/p_{N2} (N>50 at.%), it is possible that the targets are already poisoned; this would also explain the low deposition rate for this coating (as can be seen in Fig. 2). By increasing the oxygen flow, the oxygen behaviour is not linear, for lower flow rates dissociation of the oxygen molecules can occur, which increases the reactivity of the system and thus the deposition rate (seen in Fig. 2). At the same time some nitrogen atoms are replaced by oxygen ($p_{O2}/p_{N2}=0.6$) and in a second phase, the reaction between the oxygen in the target commences. This reaction starts in a monolayer formed by chemisorption and for each oxygen atom incorporated in the target, two of nitrogen are freed, due to the formation of a TiN layer or the formation of a TiO_2 layer. This will increase the partial pressure of nitrogen in the reactive atmosphere, which can explain the lower oxygen content for the coating deposited at $p_{O2}/p_{N2}=0.8$, keeping in mind that, the flow of reactive gas is always the same and so, the number of molecules of O_2+N_2 is constant. To reduce oxygen poisoning,

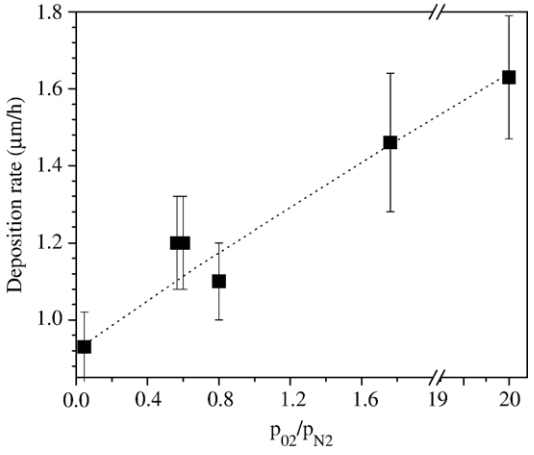

Fig. 2. Variation of the deposition rate as a function of p_{O2}/p_{N2}.

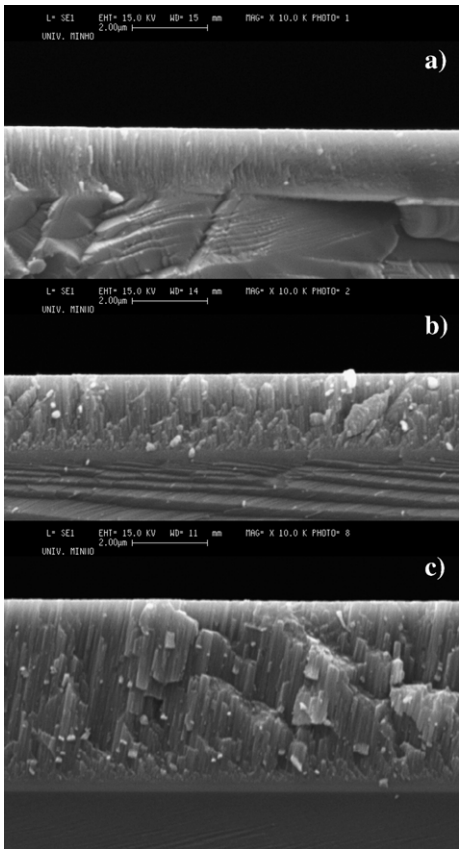

Fig. 3. Cross-sectional micrographs of Ti–Si–C–ON coatings for different p_{O2}/p_{N2} a) 0.046 b) 1.73 c) 20.

it is required to double the number of atoms in comparison to that of nitrogen. This will increase of the non-poisoned fraction of the target, according the Berg's Model, and should increase in the number of the sputtered Ti atoms, leading to an increase in Ti composition. For the coatings deposited with a high p_{O2}/p_{N2} ratio, the continuation of the previously described phenomenon occurs, but because of the decrease of the nitrogen flow, the amount of nitrogen in the coating reduces, while at the same time the oxygen flow is increased, which will promote an increase of the oxygen in the coating. The amount of oxygen added to the reactive atmosphere is not enough to reach the stoichiometric composition TiO_2, see composition of the coating deposited with $p_{O2}/p_{N2}=20$, this is an evidence of a non-poisoned target, during the deposition with high amount of oxygen, and this is the explanation for the high deposition rate of this coating, as is seen in Fig. 2.

The morphology of the coatings is disclosed by cross-sectional SEM micrographs of fractured samples, shown in Fig. 3. Considering the results for samples representing the group deposited with low p_{O2}/p_{N2} (Fig. 3a), all films show dense and very compact featureless morphologies. The decrease in the deposition rate can induce this compact morphology. The microstructure of single-phase films is qualitatively well described by the structural zone models developed by Movchan and Demchishin [14] and Thornton [15]. These models, however, change markedly when impurities or selected additives are incorporated in the films [16]. Impurities or additives (like oxygen in our case) stop the grain growth and stimulate a renucleation of grains, which results in a globular morphology. The sample deposited with $p_{O2}/p_{N2}=1.76$ (Fig. 3b) presents this type of morphology. As the p_{O2}/p_{N2} is further increased the coatings present morphologies with a large number of voids within shaped crystallites (Fig. 3c), as a result of the higher deposition rate.

3.2. Structure characterization

The differences in the composition are well correlated with the differences observed in the developed structure. The X-ray diffractograms of the as-deposited samples are illustrated in Fig. 4. International Centre for Diffraction Data (ICDD) of α—Ti (ICDD card nr. 44-1294), TiN (ICDD card nr. 38-1420, TiC (ICDD card nr. 01-071-6256), and $TiC_{0.2}N_{0.8}$ (ICDD card nr. 01-076-2484) were also included at the top of Fig. 4. The above-mentioned regimes changes (low p_{O2}/p_{N2} ratio and high p_{O2}/p_{N2} ratio) are also evident in the structural features revealed by the XRD results. For the samples deposited under low p_{O2}/p_{N2} it is possible to identify a fcc type structure and there is a tendency for an increase in the peak intensity ratio $I_{(111)}/(I_{(111)}+I_{(200)}$ with increase in p_{O2}/p_{N2}, indicating a preferential crystalline growth change. It is difficult to unequivocally identify which phases are formed. E.V. Shalaeva et al. [17] stated for Ti–Si–N–O films that at a silicon content of 10 at. %, the films had nearly single-phase crystalline structure TiSiN(O) with minimum grain size 1.5–2 nm. Although, at that moment, with the diffraction analysis, there is no evidence that silicon is partially dissolved in a cubic solid solution TiSiN(O). Carbon and oxygen substitution of regular nitrogen positions to formed fcc Ti(C,O,N) phase, once the nitrogen content decreases, could be possible. The samples that were deposited at high p_{O2}/p_{N2} presented a significant loss of crystallinity, with the sample with highest oxygen content found to be amorphous. For this group the increase in the deposition rate (as mentioned before) and the available oxygen that is incorporated in the lattice, reduces the possibility of crystallization. The extended deformation of the fcc structure resulting from the

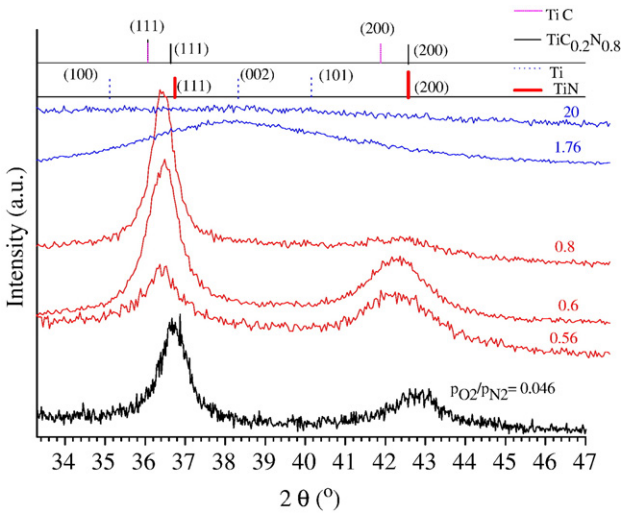

Fig. 4. XRD patterns for different Ti–Si–C–ON films.

incorporation of oxygen probably increases the number of defects, which facilitates the formation of the amorphous structure. The observed changes in film structure and orientation as a function of p_{O2}/p_{N2}, can be described in three steps:

- First at low p_{O2}/p_{N2}, the oxygen is probably incorporated into the grain boundaries and continues to accumulate during GB migration, resulting in a texture with low degree of preferred orientation and with low grain size (Fig. 4);
- Second with slightly higher p_{O2}/p_{N2} coarsening during coalescence is severely suppressed. The competitive growth which follows is governed by anisotropic crystallographic effects since the oxygen is incorporated into the lattice, as described in [18]. The film is composed of globular grains (Fig. 3b) with random orientation (Fig. 4);
- Third as the p_{O2}/p_{N2} is further increased, with increasing oxygen concentration, the grain size decreased. The presence of oxide phases inhibits GB migration in the bulk of the film, preventing grain coarsening, becoming the film growth, at very high p_{O2}/p_{N2}, amorphous.

3.3. Mechanical properties

The evolution of hardness and Young's modulus as a function of the p_{O2}/p_{N2} is illustrated in Fig. 5. The structural changes are consistent with the evolution of the hardness, as it can be seen by the significant reduction of the hardness by increasing p_{O2}/p_{N2}, varying from typical TiN (23 GPa) film for the lowest p_{O2}/p_{N2} to those of TiO_x amorphous phase for highest concentration of oxygen (≈15 GPa) [19]. The replacement of nitrogen by carbon atoms and the addition of Si in the coatings leads to a distortion in the NaCl lattice type structure, which usually results in the increase of hardness [20,21]. This is not observed in our coatings probably due to the amount of oxygen, as it is known that the oxygen acting as an impurity decreases the hardness of the coatings [22]. A visible decrease in Young's modulus was found, with increasing p_{O2}/p_{N2} and relates to an increase on the defect density and also the decrease of the bonding energy, due to the increase distance between the atoms Ti, N and O, as the structure changes to an amorphous type.

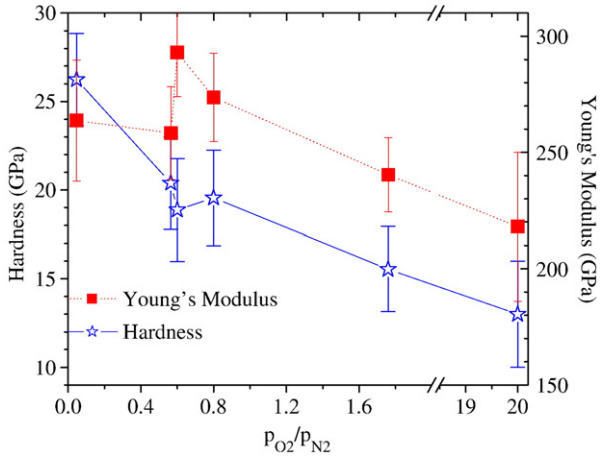

Fig. 5. Hardness of sputtered Ti–Si–C–ON as a function of p_{O2}/p_{N2}.

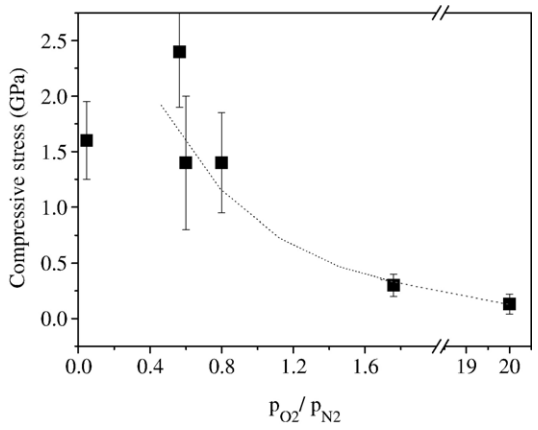

Fig. 6. Compressive residual stresses of sputtered Ti–Si–C–ON as a function of p_{O2}/p_{N2}.

Fig. 6 shows the evolution of residual stress as function of p_{O2}/p_{N2}. From this graph it is clear that all coatings are in the compressive stress state. This result should be expected because of the low working pressure (<0.45 Pa). Under these conditions, sputtered atoms or reflected Ar neutrals could induce the well-known atomic peening effect, which promotes the compressive residual stress state [12,23]. Regarding the evolution of the compressive stresses with increasing p_{O2}/p_{N2}, it is possible to see that there is a dependence of the residual stress on the p_{O2}/p_{N2}. It is also noticeable a correlation between the compressive stresses and the measured hardness. First the hardest samples (deposited with low p_{O2}/p_{N2}) presented the highest residual stress values, which we believe is due to film densification and the presence of lattice defects in the film's structure, which act as an obstacle for dislocation motion. Secondly, for the films deposited with a high p_{O2}/p_{N2} which presented very low hardness values and developed a porous columnar growth is observed a strong tendency for stress reduction. Furthermore, as the oxygen increases the distortion in the crystalline lattice increases, leading to a tendency for film to become amorphous, as can be seen from the diffraction patterns. As a result of this higher degree of amorphous structure, the films enhance their capacity to accommodate the stress, leading to a reduction of its value. For the highest oxygen content, reached for highest p_{O2}/p_{N2}, the coating is amorphous and therefore the residual stresses and hardness are very low. In the literature, Parreira et al. [12] as well as Vaz et al. [19] have studied the influence of the oxygen fraction in the residual stresses and hardness of W–O–N, Ti–O–N coatings, respectively. Globally, also their case, the hardness and residual stress decreased with increasing oxygen fraction.

4. Conclusions

Ti–Si–C–ON thin films were deposited by reactive magnetron sputtering with different p_{O2}/p_{N2}. The films deposited under low p_{O2}/p_{N2} presented a dense and compact morphology, a fcc—cristalline structure, hardness higher than 20 GPa, higher

compressive residual stress. The films that were deposited with higher p_{O2}/p_{N2} presented a porous morphology and are amorphous. These samples exhibited low hardness and very low compressive residual stress. Tanking account the application of these coatings (biomedical application), preliminary results showed, that samples deposited with higher ratios of p_{O2}/p_{N2} presented lower values of biofilm formation, indicating that the increase of oxygen leads to biomaterials less susceptible to be colonized by *S. epidermidis*. However, these bioassays will be presented by the authors in a future publication.

References

[1] D.V. Stansky, D.V. Levashov, N.B. Glushankova, N.B. D'yakonova, et al., Surf. Coat. Technol. 182 (1) (2004) 101.
[2] Kalpana S. Katti, Colloids Surf. B Biointerfaces 39 (2004) 133.
[3] Nuno Cerca, Sílvia Martins, Gerard B. Pier, Rosário Oliveira, Joana Azeredo, Res. Microbiol. 156 (2005) 650.
[4] M. Henriques, J. Azeredo, R. Oliveira, Br. J. Biomed. Sci. 63 (1) (2006) 5.
[5] B. Jansen, K. Kristinsson, S. Jansen, G. Peters, G. Pulverer, J. Antimicrob. Chemother. 30 (1992) 135.
[6] S. Vepřek, A. Nioderhofer, K. Moto, et al., Surf. Coat. Technol. 133–134 (2000) 152.
[7] F. Vaz, P. Cerqueira, L. Rebouta, S.M.C. Nascimento, E. Alves, Ph. Goudeau, J.P. Rivière, Surf. Coat. Technol. 174–175 (2003) 197.
[8] E. Ariza, L.A. Rocha, F. Vaz, L. Cunha, S.C. Ferreira, P. Carvalho, L. Rebouta, E. Alves, Ph. Goudeau, J.P. Rivière, Thin Solid Films 469–470 (2004) 274.
[9] C. Lopes, N.M.G. Parreira, S. Carvalho, A. Cavaleiro, J.P. Rivière, E. Le Bourhis, F. Vaz, Surf. Coat. Technol. 201 (2007) 7180.
[10] D.P. Dowling, P.V. Kola, K. Donnelly, T.C. Kelly, K. Brumitt, L. Lloyd, R. Eloy, M. Therin, N. Weill, Diamond Relat. Mater. 6 (1997) 390.
[11] J.M. Antunes, A. Cavaleiro, L.F. Menezes, M.I. Simões, J.V. Fernandes, Surf. Coat. Technol. 149 (2002) 27.
[12] N.M.G. Parreira, N.J.M. Carvalho, F. Vaz, A. Cavaleiro, Surf. Coat. Technol. 200 (2006) 6511.
[13] G.G. Stoney, Proc. Roy. Soc. 82 (1909) 172 (London) [A].
[14] B.A. Movchan, A.V. Demchishin, Fizita Metall. 28 (1969).
[15] J.A. Thornton, Ann. Rev. Mater. Sci. 7 (1977) 239.
[16] P. Barna, M. Adamik, in: Y. Pauleau, P.B. Barna (Eds.), Protective Coatings and Thin Solid Films, Kluwer Academic Publisher, 1997.
[17] E.V. Shalaeva, S.V. Borisov, O.F. Denisov, M.V. Kuznetsov, Thin Solid Films 339 (1999) 129.
[18] I. Petrov, P.B. Barna, L. Hultman, J.E. Greene, J. Vac. Sci. Technol. A. 21 (5) (2003) S117.
[19] F. Vaz, P. Cerqueira, L. Rebouta, S.M.C. Nascimento, E. Alves, Ph. Goudeau, J.P. Rivière, K. Pisschow, J. de Rijk, Thin Solid Films 447–448 (2004) 449.
[20] M. Stueber, P.B. Barna, M.C. Simmonds, U. Albers, H. Leiste, C. Ziebert, H. Holleck, A. Kovács, P. Hovsepian, I. Gee, Thin Solid Films 493 (2005) 104.
[21] F. Vaz, L. Rebouta, S. Ramos, A. Cavaleiro, M.F. da Silva, J.C. Soares, Surf. Coat. Technol. 100–101 (1998) 110.
[22] S. Vepřek, H.-D. Männling, A. Niederhofer, D. Ma, S. Mukherjee, J. Vac. Sci. Technol. B. 22 (2) (2004) L5 (Mar.–Apr.).
[23] M. Ohring, The Materials Science of Thin Films, Academic Press, San Diego, 1992.